Study on Short-term DC Breakdown and Corona-resistance Mechanism of Polyimide

Dongri Xie, Chenyu Yan, Yin Huang, Daomin Min*, Shengtao Li*
State Key Laboratory of Electrical Insulation and Power Equipment, Xi'an Jiaotong University, Xi'an, 710049, China
*E-mail: forrestmin@mail.xjtu.edu.cn and sli@mail.xjtu.edu.cn

***Abstract*—Nano-doping has a significant effect on dielectric and electrical insulation for polymer dielectrics. Pure polyimide 100HN and nano-doping polyimide 100CR from DuPont Company are adopted to conduct short-term breakdown and long-term corona-resistant experiments. The results show that, the short-term breakdown strength of 100CR is 6.4% lower than 100HN. For long-term corona resistance, the corona-resistant time of 100CR is 400% longer than 100HN. In order to study the influencing mechanism of nanoparticles on short-time breakdown and long-term corona resistance, isothermal surface potential decay experiments were conducted to investigate traps characteristics of two samples. It is found that the traps energy and density of 100CR is less than that of 100HN. The volume conductivity of 100CR is much higher than 100HN. The eroded surface morphologies of 100HN and 100CR are observed by Scanning Electron Microscope, which are groove channels and different eroded layered rings respectively. The results show that the effect of nanoparticles on short-term breakdown and long-term corona resistance are different. For short-term breakdown, the main consideration is the change of traps and conductance changed by nano-doping. For long-term corona-resistance, the collision scattering effect of nanoparticles against the charged particles plays the dominate role.**

Keywords: Breakdown, corona-resistance, traps, morphology, collision scattering

I. INTRODUCTION

Polymer dielectric breakdown in electrical equipment is a catastrophic failure. The development of nanotechnology provides new ideas and solutions for the development of dielectric insulation materials for higher voltage levels and complex operating conditions [1-2].

In previous work, it is experimentally found that the breakdown strength exists a maximum value at a low content of nano-doping [3], while the corona-resistance performance increases linearly with the nano-doping content increasing [4]. Until now, dielectric breakdown and corona-resistance processes in nanocomposites are still not clear, especially the role of nanoparticles in which to play, it has not yet formed a unified point of view [5-8]. But it is widely accepted that the space charge transport in dielectrics is closely related to dielectric and electrical performance [6-8]. The physical and chemical properties of the interface region after nano-doping strongly affect the charge transport process [6], which leading to the change of electrical performance. T. Tanaka [7]et al proposed the multi-core model of the interface region and zigzag discharge path, the extending discharge path enhanced the corona resistance. Furthermore, space charge modulated dielectric breakdown by simulated method [9-10] had further made the electric field increasing process in dielectrics clearer.

This work was supported by the National Basic Research Program of China (973 Program) under Project with No. 2015CB251003, the National Natural Science Foundation of China (NSFC) under Project with No. 51337008.

In this paper, the charge dissipation characteristics and traps parameters were analyzed by isothermal surface potential decay (ISPD), combined with volume conductivity and SEM observed morphology after corona discharge, the effect of nanoparticles on short-term dc breakdown and long-term corona-resistance is further clear.

II. EXPERIMENTAL METHOD

2.1 Broadband dielectric relaxation

The broadband dielectric relaxation experiments were carried out on 100HN and 100CR samples by Novocontrol broadband dielectric spectroscopy (Concept80). Ac voltage of 1 V was applied on the sample at 25°C. The frequency ranges from 10^{-1}-10^{6} Hz.

2.2 Scanning Electron Microscope

The eroded surface morphology of 100HN and 100CR after the corona discharge were observed by spraying gold at the surface of the eroded samples by VE9800S Scanning Electron Microscope (SEM).

2.3 Volume resistivity

The volume resistivity of 100HN and 100CR were tested by Keithley 6517B volume resistivity test system. The fixed 500V DC voltage was applied on the dielectric, and the tiny current flowing through the dielectric was measured to calculate the volume resistivity. Each sample is measured 8 times, respectively.

2.4 Isothermal surface potential decay

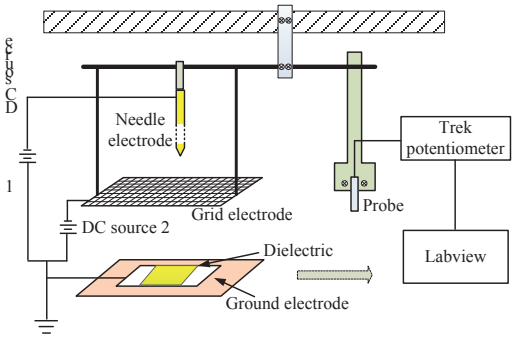

Figure 1. ISPD device diagram

To deposit a certain amount of charge on the dielectric surface by needle-grid corona-charge, the decay of dielectric surface potential after corona-charge reflects the charge dissipation characteristics and the traps characteristics. The ISPD experimental device diagram is shown in Figure 1. The voltage applied on the needle electrode is the charging voltage; the voltage applied on the grid is the grid voltage. The charging voltage and the grid voltage are -15kV and -5kV, respectively. The charging time is 3 minutes. After the corona-charge, the surface potential of the dielectrics began

to decrease. Immediately, TREK® surface potentiometer probe was moved to the charging point on the dielectric surface. The dielectric surface potential with time was recorded. The experiment was carried out in a thermostatic glass box with an experimental temperature of 25°C and the air relative humidity of 40%.

2.5 Short-term dc breakdown

100CR and 100HN polyimide films with the same thickness of 25μm were used to conduct short-term dc breakdown experiment. The spherical copper electrode diameter is 25mm and DC breakdown is tested in transformer oil at 25°C. The voltage applied on the dielectric was linearly boosted at a rate of 1 kV/s until the breakdown occurs, and the recorded voltage was used as the breakdown voltage of the sample. Breakdown voltages were recorded 18 times, respectively.

2.6 Corona-resistance

For the needle-plate electrode system, electric field at the tip of the needle is the highest. When the applied voltage on the needle increases to a certain value, corona discharge occurs at the needle tip. Corona discharge produces large amount of charged particles that directly collide with the polymer matrix to cause damage of the polymer chains [11]. The fixed AC 5kV is used to conduct corona-resistance test at 25°C. The distance between the needle tip and the upper surface of polyimide is 2.55mm. The corona-resistance test system diagram and experimental diagram are shown in Figure 2. Under the applied constant voltage, the corona-resistant time from test begin to the occurrence of breakdown were recorded. 100CR and 100HN were tested for 9 times, respectively.

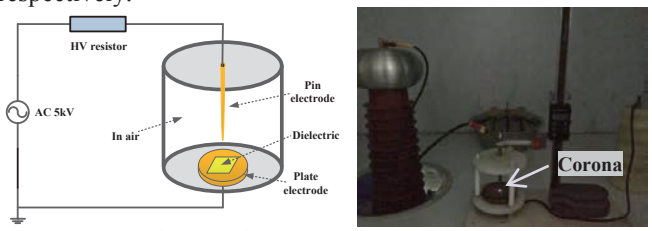

Figure 2. The corona-resistant test system

III. Experiment Results and Analysis

3.1 Broadband dielectric relaxation

The relative real permittivity ε' of 100HN and 100CR was shown in Figure 3.

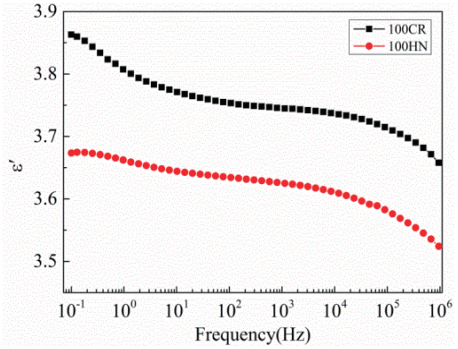

Figure 3. Relative real permittivity of 100CR and 100HN

By contrasting the broadband dielectric spectra, ε' of 100CR can be seen obviously increased compared with 100HN. For the nanocomposite dielectric, the physical and chemical properties of the polymer matrix, inorganic nanoparticles and the interface zone between the nanoparticles and matrix are different [7]. Each part is likely to cause a different polarized process. The introduced nanoparticles have a larger dielectric constant relative to the polymer matrix. The high dielectric constant of inorganic nanoparticles leads to the dielectric constant increase of the nanocomposite.

3.2 Volume resistivity

The measured volume resistivity of 100CR and 100HN are 5.24×10^{15} and 5.22×10^{16} Ω•cm, respectively. The volume resistivity of nanocomposite polyimide 100CR is reduced by 10 times compared to pure polyimide 100HN.

3.3 Isothermal surface potential decay

The equations of traps energy and traps density can be obtained by Simmons theory[12].

$$E_T = k_B T \ln(\upsilon_{ATE} t) \quad (1)$$

$$Q_s(t) = t\frac{\varepsilon_0 \varepsilon_r}{q_e L}\frac{d\phi_s(t)}{dt} \quad (2)$$

where, E_T is the trap energy; k_B is the Boltzmann constant; T is the temperature; $\upsilon_{ATE}=k_BT/h$, h is the Planck constant; $Q_s(t)$ is the trapped charge density; ε_0 is the vacuum dielectric constant; ε_r is the relative permittivity of polyimide; q_e is the element charge; L is the sample thickness; $\phi_s(t)$ is the initial surface potential, t is the potential decay time.

The ISPD test results of 100HN and 100CR are shown in Figure 4. Combined with the double-trap model, the double-exponential curve fitting of the measured surface potential decay data is carried out. And the traps energy and density can be obtained according to equations (1) and (2). Drawing the E_T-$Q_s(t)$ curve, the traps distributions of 100CR and 100HN are shown in Figure 5.

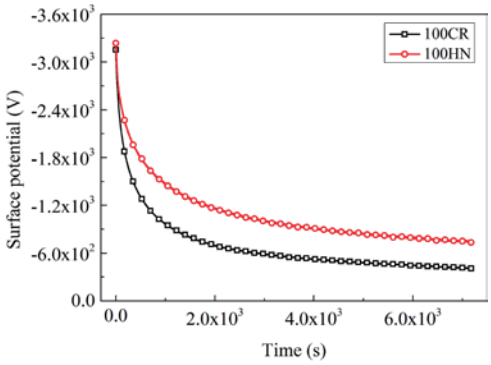

Figure 4. ISPD test results

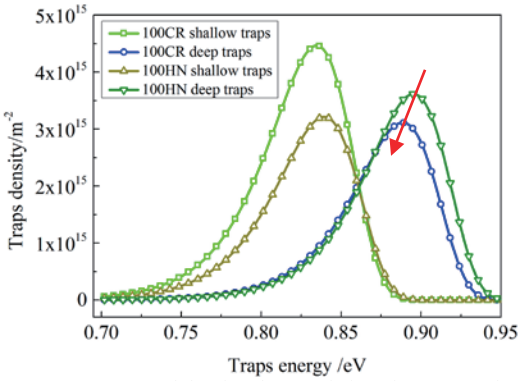

Figure 5. Trap energy and density characteristics of 100HN and 100CR

Seen from Figure 4, at the same initial surface potential of 100CR and 100HN, the potential decay rate of 100CR is

much faster. Seen from Figure 5, the deep traps energy and density of 100CR is reduced compared with 100HN, as shown the direction of arrow.

3.4 Short-term dc breakdown

The results of breakdown strength and the failure time of polymer dielectrics satisfy the Weibull statistical distribution. According to the short-term breakdown experimental results, the obtained Weibull distribution is shown in Figure 6. The relationship of $\ln E_b$-$\ln\ln(1/(1-F))$ diagram is the Weibull distribution. The scale parameter α and the shape parameter β are shown in Table 1. Meanwhile, α is the scale parameter, that is, the breakdown strength value when the breakdown probability is 63.2%, kV/mm, or the corona-resistant time, s; β is the shape parameter, indicating the degree of dispersibility of the experimental results.

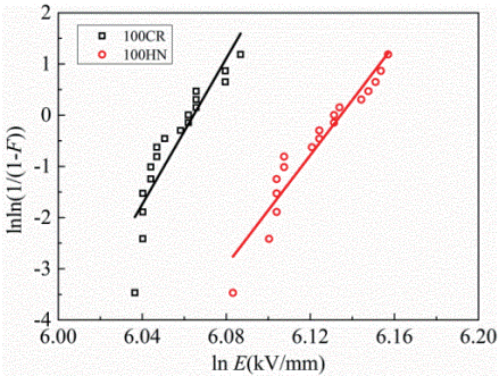

Figure 6. The Weibull distribution of short-term breakdown

Table I. The Weibull parameters of short-term breakdown

Sample	Weibull parameter	
	α (kV/mm)	β
100CR	430.8	43.6
100HN	460.3	45.9

From the obtained Weibull parameters, it can be seen that the dc breakdown strength of nano-doping polyimide 100CR is 6.4% lower than that of pure polyimide 100HN.

3.5 Corona-resistance

The obtained Weibull distribution of $\ln t$-$\ln\ln(1/(1-F))$ is shown in Figure 7. The scale parameter α and the shape parameter β are shown in Table 2.

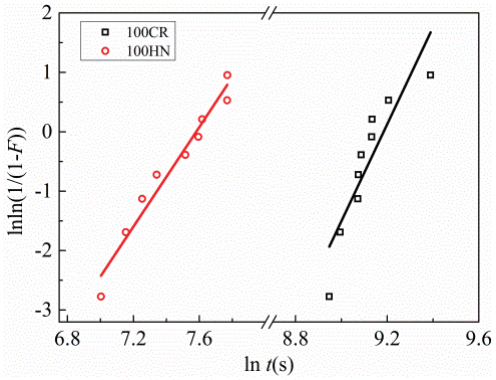

Figure 7. The Weibull distribution of long-term corona-resistance

Table II. The Weibull parameters of long-term corona-resistance

Sample	Weibull parameter	
	α (s)	β
100CR	9745	8.2
100HN	1960	4.2

From the obtained Weibull parameters, it can be seen that the long-term corona-resistance of nano-doped polyimide 100CR is about 400% higher than that of pure polyimide 100HN.

3.6 Eroded morphology after corona discharge

The eroded surface morphology characteristics of 100HN and 100CR after the corona discharge until breakdown occurrence were intuitively observed to be completely different, as shown in Figure 8. The eroded area of pure polyimide 100HN is clearly less than 100CR. Besides, 100CR presents layered rings morphology.

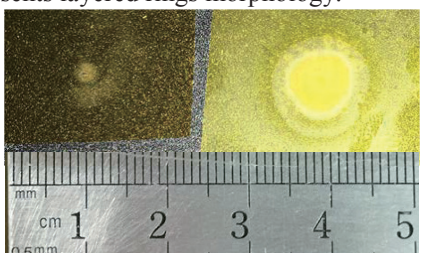

100HN 100CR

Figure 8. Surface morphology after corona discharge

Further observation of the surface morphology after corona discharge by SEM is conducted, as shown in Figure 9. For 100CR, 50 magnification of SEM observation revealed that a significant different eroded degree from the center to outside. Besides, the central layer of erosion is the most serious; the outer layer eroded degree is weaker. For 100HN, the eroded surface morphology is a "groove channel", the groove is basically linear, and the breakdown point exists in the middle of the groove, which is under the tip of the needle.

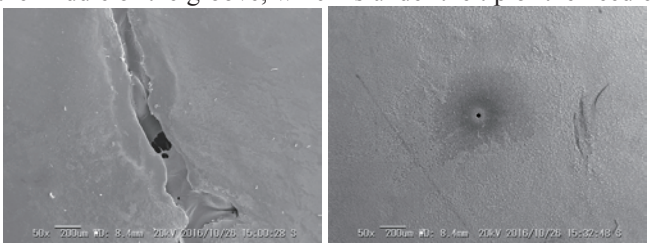

100HN 100CR

Figure 9. SEM of eroded surface morphology

IV. SHORT-TERM BREAKDOWN AND CORONA-RESISTANCE ANALYSIS

Obviously, the short-term breakdown strength of 100CR was 6.4% lower than that of 100HN, while the long-term corona resistance of 100CR was improved by about 400% than that of 100HN. Hence, the big difference shows that nano-dopants may act as the different roles in short-term breakdown and long-term corona-resistant process.

4.1 Short-term breakdown analysis

Due to the huge specific surface area of nanoparticles, the interactive region structure is formed between the nanoparticle and polymer matrix. The introduction of nanoparticles change the polarization and traps characteristics of nanocomposite [7-8], which further affects the space charge transport, dielectric behavior and conductance characteristics of polymer dielectrics. It is generally believed that the dc dielectric breakdown performance of nanocomposite reaches to the maximum value at a relative low nano-doping content [8]. However, when the nano-doping content exceeds a certain value, the formed interactive regions will have an overlapping, which is of beneficial to the carriers' migration and the corresponding dielectric breakdown performance is reduced. It is believed

that the traps characteristics play a vital role in dielectric breakdown with different nano-doping content [13].

The charge transport and free volume breakdown model [9] is shown in Figure 10. Under high electric field, electrons and holes are injected into the insulating material from electrodes. The obtained maximum energy $eF_{max}\lambda$ gained at the free volume zone is corresponding to the maximum local electric field F_{max} in the migration process. When the maximum energy $eF_{max}\lambda$ of carriers exceeds the traps potential barrier E_T, the trapped carriers can go over the potential barrier and go further migration. If the traps energy and density is reduced, the trapping effect is reduced, carriers can migrate more unobstructed, and thus, the carrier multiplication process at applied high field strength is easier to form, finally leading to the occurrence of breakdown.

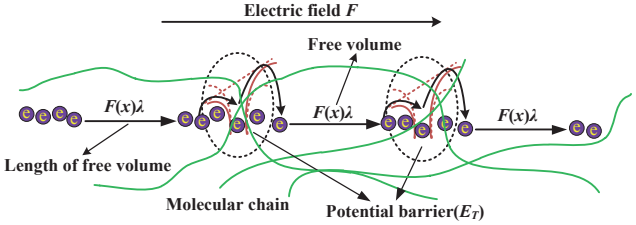

Figure 10. The charge transport and free volume breakdown model

Based on the analysis above, the energy or density increase of deep traps can reduce the carriers' energy and make it harder for the carriers to go over the potential barrier [13]. As a consequence, the local carriers and current multiplication are difficult to form. For the short-term breakdown properties of 100HN and 100CR, seen from the traps parameters, the deep traps energy and density of 100CR is decreased compared with 100HN. So that the trapping effect becomes weaker and the carriers can go over the potential barriers with more probability and ability, which increases the carriers' multiplication process and the volume conductivity [14]. As a consequence, the conductive path in polyimide 100CR is easier formed than 100HN. Based on the analysis above, the association between traps characteristics, conductance, and short-term breakdown performance is further clear.

4.2 Corona-resistance model and analysis

When the corona discharge occurs on the surface of the polymer insulating material, the charged particles, oxygen and nitrogen plasma, ultraviolet light and thermal effect can directly erode the polymer matrix [11], causing the degradation and destruction of the polymer matrix until local damage is initiated The established corona-resistant model of 100HN and 100CR are shown in Figure 11.

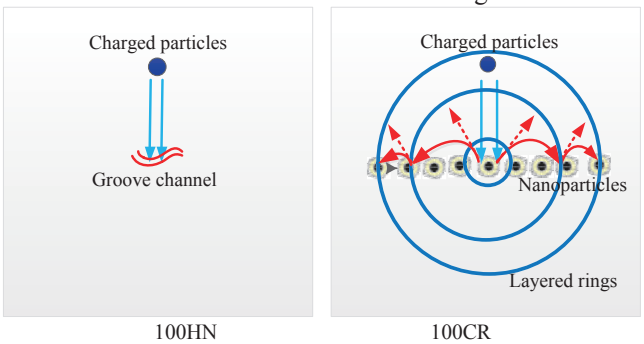

Figure 11. Corona-resistance models of 100HN and 100CR

For pure polyimide 100HN, the eroded surface morphology is a "groove channel". The charged particles collide directly with the polymer matrix when corona occurs. The energy of the charged particles is directly transferred to the polymer matrix continuously until it is enough to break the molecular chain. And the charged particles migrate along the surface from inside to outside along the surface. Owing the deeper traps have bigger potential barrier. In the region with more shallow traps, the bigger probability the carriers migrate towards. The charged particles migrate along the shallower traps on the surface. Meanwhile, the recombination of electron-positive ion pairs and positive and negative ions pairs can release energy [11,15], which resulting in local polymer molecular chain breaks. Therefore, the recombination process of the charged particles occurs more in the region along the shallower traps, causing the local molecular chain to break. And thus continuously, a "groove channel" is formed.

While for polyimide 100CR, the eroded surface morphology is a "layered rings". Firstly, the dielectric constant of the inorganic nanoparticles is higher than that of organic polymer matrix. When corona begins, the charged particles are more concentrated in the inorganic particles [16]. Owing the nanoparticle has a large collision coefficient compared with the polymer matrix. When the charged particles collide with the polymer surface, part energy of the charged particles is transferred to the polymer matrix, leading to the break of the molecular chains. Considering the existence of large amount of hard nanoparticles, collision scattering is more likely to occur when the charged particles collide with the nanoparticles on the surface of the sample. So the polymer matrix in the area below the needle tip can be partly protected compared with 100HN. The energy of original charged particles is partly transferred to the polymer matrix and the residual energy is used for the continuous movement. Due to the collision scattering effect against the charged particles, the charged particles are scattered to the outside area. Some charged particles secondarily collide with the polymer surface, and the outer collided region is also damaged. Thus, the outer eroded ring is formed. The residual energy of the charged particles in this process is smaller than the energy of the charged particles emitted from the needle tip. So the eroded degree after the scattering is reduced. After the scattering effect of the nanoparticles, charged particles undergo multiple collisions with the sample surface, resulting in a distinct "layered rings morphology with different eroded degree".

Furthermore, the introduction of large quantities of nanoparticles causes the traps energy and density of 100CR shallower, which accelerates the charge dissipation as shown in ISPD experiments, thus reducing the electric field stress concentration. It is auxiliary to improve the corona resistant performance. It should be noted that the scattering effect of the nanoparticles plays a dominate role in the improvement of the corona resistance of 100CR when the nano-doping content is high. Thus, synergistic collision scattering and charge dissipation effect is proposed to interpret the occurrence of different eroded layered rings and the better corona-resistance.

V. CONCLUSION

(1) The short-term dc breakdown performance of 100CR decreased by 6.4% compared with 100HN. The introduction of large quantities of nanoparticles cause

shallower traps energy and density, which decreases the trapping effect, the carrier can migrate further by going over less potential barrier, leading to the increased mean free path, carrier mobility and energy. The carrier multiplication process at high field strength is easier to form, thus reducing the dc breakdown strength.

(2) The corona-resistant performance of 100CR is increased by about 400% than 100HN. Collision scattering is mainly considered to interpret the occurrence of different eroded layered ring and the better corona-resistance when nano-doping content is high. Besides, the accelerated dissipation of charged particles is auxiliary to improve the corona-resistance performance.

REFERENCE

[1] T. Tanaka, G. C. Montanari, and R. Mulhaupt, "Polymer nanocomposites as dielectrics and electrical insulation-perspectives for processing technologies, material characterization and future applications," IEEE Trans. Dielectr. Electr. Insul. Vol. 11, pp. 763-784, 2004.

[2] S. Li, S. Yu, and Y. Feng, "Progress in and prospects for electrical insulating materials," High Volt. Vol. 1, pp. 122-129, 2016.

[3] S. Li, G. Yin, G. Chen, J. Li, S. Bai, L. Zhong, Y. Zhang, and Q. Lei, "Short-term breakdown and long-term failure in nanodielectrics: A review," IEEE Trans. Dielectr. Electr. Insul. Vol. 17, pp. 1523-1535, 2010.

[4] M. Chen, J. Yin, D. Song, X. Liu, Y. Feng, and B. Su, "Fabrication and Characterization of Polyimide/AlN Nanocomposite Films," Polym. Polym. Compos. Vol. 22, pp. 221-226, 2014.

[5] T. J. Lewis, "Nanometric dielectrics," IEEE Trans. Dielectr. Electr. Insul. Vol. 1, pp. 812-825, 1994.

[6] J. K. Nelson, and J. C. Fothergill, "Internal charge behavior of nanocomposites," Nanotechnology. Vol. 15, pp. 586-595, 2004.

[7] T. Tanaka, M. Kozako, N. Fuse, and Y. Ohki, "Proposal of a multi-core model for polymer nanocomposite dielectrics," IEEE Trans. Dielectr. Electr. Insul. Vol. 12, pp. 669-681, 2005.

[8] S. Li, G. Yin, S. Bai, and J. Li, "A new potential barrier model in epoxy resin nanodielectrics," IEEE Trans. Dielectr. Electr. Insul. Vol. 18, pp. 1535-1543, 2011.

[9] S. Li, D. Min, W. Wang, and G. Chen, "Modelling of dielectric breakdown through charge dynamics for polymer nanocomposites," IEEE Trans. Dielectr. Electr. Insul. Vol. 23, pp. 3476-3485, 2017.

[10] G. Chen, J. Zhao, S. Li, and L. Zhong, "Origin of thickness dependent dc electrical breakdown in dielectrics," Appl. Phys. Lett. Vol. 100, pp. 222904:1-4, 2012.

[11] S. Akram, G. Gao, Y. Liu, J. Zhu, G. Wu, and K. Zhou, "Degradation mechanism of Al_2O_3 nano filled polyimide film due to surface discharge under square impulse voltage," IEEE Trans. Dielectr. Electr. Insul. Vol. 22, pp. 3341-3349, 2016.

[12] Q. Lei, F. Tian, C. Yang, L. He, and Y. Wang, "Modified isothermal discharge current theory and its application in the determination of trap level distribution in polyimide films," J. Electrost. Vol. 68, pp. 243-248, 2010.

[13] W. Wang, D. Min, S. Li, "Understanding the conduction and breakdown properties of polyethylene nanodielectrics: effect of deep traps," IEEE Trans. Dielectr. Electr. Insul. Vol. 23, pp. 564-572, 2016.

[14] K. Wu, L. A. Dissado, and T. Okamoto, "Percolation model for electrical breakdown in insulating polymers," Appl. Phys. Lett. Vol. 85, pp. 4454-4456, 2004.

[15] K. C. Kao, "New theory of electrical discharge and breakdown in low mobility condensed insulators," J. Appl. Phys. Vol. 55, pp. 752-755, 1984.

[16] Z. Li, K. Okamoto, Y. Ohki, and T. Tanaka, "Effects of nano-filler addition on partial discharge resistance and dielectric breakdown strength of Micro-Al_2O_3/Epoxy composite," IEEE Trans. Dielectr. Electr. Insul. Vol. 17, pp. 653-661, 2010.